

# Learning to Simulate Human Movement

Hua Wei<sup>1</sup> and Zhenhui Li<sup>1</sup>

<sup>1</sup>The Pennsylvania State University

<sup>1</sup>{hzw77, jessieli}@ist.psu.edu

December 4, 2021

## Abstract

The simulation of human movement on the space is useful for policy-making in transportation, public safety, and public health. The human movements can be viewed as a dynamic process that human transits between states (*e.g.*, locations) over time. In the human world where both intelligent agents like humans or vehicles with human drivers play an important role, the states of agents mostly describe human activities, and the state transition is influenced by both the human decisions and physical constraints from the real-world system (*e.g.*, agents need to spend time to move over a certain distance). Therefore, the simulation of human movements should include the modeling of the agent’s decision process and the physical system dynamics. In this paper, we propose *MoveSD* to learn to simulate human movement through learning decision model and integrating system dynamics. In experiments on real-world datasets, we demonstrate that the proposed method can achieve superior performance against the state-of-the-art methods in simulating the human movements.

## 1 Introduction

The simulation of human movement on space is useful for policy-making in various applications, ranging from transportation [Wu et al., 2018, Lian et al., 2014], public safety [Wang et al., 2017] to public health [Wang et al., 2018]. For example, the simulation of vehicles with human drivers can serve as a foundation and a testbed for reinforcement learning (RL) on traffic signal control [Wei et al., 2018] and autonomous driving [Wu et al., 2018]. In fact, lacking a good simulation is considered as one of the key challenges that hinder the application of RL in real-world systems [Dulac-Arnold et al., 2019].

The simulation of human movements on space can be viewed as modeling the state transition of intelligent agents (*e.g.*, human travelers, or vehicles with human drivers). The state of an agent can include its historical locations and its destination. Recently there are growing research studies that have developed

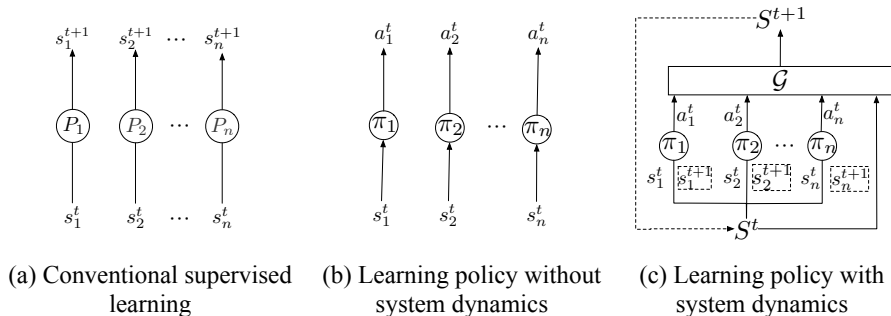


Figure 1: Three perspectives on modeling state transitions. (a) Traditional methods directly predict the next state  $s^{t+1}$  for an agent based on its past states with a model  $P$ . (b) Direct learning of agent policy  $\pi$  that maps from state  $s$  to action  $a$ . (c) Learning agent policy  $\pi$  with the system dynamics  $\mathcal{G}$ . The agents observe its state  $s^t$  from the system state  $S^t$ , which is modeled by the system dynamics model  $\mathcal{G}$ .

computational methods to learn to simulate from the state transitions. One line of research is to use supervised learning methods which directly predict the next states based on current state and historical states [Song et al., 2016, Liu et al., 2016, Feng et al., 2017, Baumann et al., 2018, Feng et al., 2018]. As is shown in Figure 1 (a), they focus on directly minimizing the error between estimated state  $\hat{s}_{t+1}$  and true observed state  $s_{t+1}$ , with an end-to-end prediction model  $P$  for the agent. In the real world where agents can take actions and interact with each other, the state of an agent is influenced not only by its previous states, but more importantly, by its action and other agents. It would require a large number of observed states that cover the whole state distribution to learn an accurate state transition model. When the agent encounters unobserved states, and the learned model is likely to predict  $s^{t+1}$  with a large error. An example is, when a vehicle drives on the road it has never observed before, these methods would fail to predict the movements. If we know the driving policy of the vehicle (*e.g.*, the vehicle follows the shortest path to its destination), the vehicle’s movement can still be inferred.

Another line of research considers the underlying mechanism behind the state transition of movements from a decision-making perspective [Ziebart et al., 2008, Zou et al., 2018, Bhattacharyya et al., 2018, Song et al., 2018]. As shown in Figure 1 (b), they aim to learn a decision policy  $\pi$ , which can generate the movements by taking a sequence of actions  $a$  from policy model  $\pi$ . For example, imitation learning (IL) can be used to learn the routing policy of a vehicle, which aims to learn to take actions (*e.g.*, keep moving on the current road, turn left, turn right, go straight, and take U-turn) based on the current state of the vehicle (*e.g.*, the road ID, the number of vehicles and average speed on the road) [Ziebart et al., 2008]. The policy learned is more applicable to the unobserved state because the dimension of action space is usually smaller than state

space that increases exponentially with the number of state features. However, IL methods assume that the next state is purely decided by the action of the agent. In contrast, the state transition of an agent in the real world is a combined effect of agent decision and system dynamics. For example, if a driver presses the brake pedal, system dynamics determine this vehicle’s location after this action, which is mostly affected by factors such as the tires of vehicles, road surface, and weather. As another example, a person arrives at location  $A$  and want to check in, but  $A$  has a limitation in the population it can serve. So the person would have to spend time to wait. Therefore, if we ignore the fact that the policy and final state of an agent must comply with the constraints from system dynamics, it will make the learned state transition model less realistic.

With the limitations of traditional prediction methods and imitation learning methods, in this paper, we formulate the problem of state transition modeling as modeling a decision-making process and incorporating system dynamics. As shown in Figure 1 (c), we consider the state of an agent is a joint outcome of its decision and system dynamics. The agent observes state  $s^t$  from the system state  $S^t$ , takes action  $a^t$  following policy  $\pi$  at every time step. Then the system model  $\mathcal{G}$  considers current system state  $S^t$  and the actions  $\{a_1^t, \dots, a_N^t\}$  of all agents and outputs the next system state  $S^{t+1}$ , upon which the agents observe their next states  $\{s_1^{t+1}, \dots, s_N^{t+1}\}$ . This formulation looks into the mechanism behind state transitions and provides possibilities to include system dynamics in the modeling of state transitions. Specifically, we propose *MoveSD*, which utilizes a similar framework as Generative Adversarial Imitation Learning (*GAIL*) [Ho and Ermon, 2016] to model the decision process of agents, with a generator learning policy  $\pi$  and a discriminator  $\mathcal{D}$  learning to differentiate the generated movements from observed true movements. Moreover, *MoveSD* explicitly models system dynamics  $\mathcal{G}$  and its influence on the state transition through learning  $\pi$  and  $\mathcal{D}$  with the constraints from  $\mathcal{G}$  and through providing an additional intrinsic reward to  $\pi$ . Extensive experiments on real-world data demonstrate that our method can accurately predict the next state of an agent and accurately generate longer-term future states.

## 2 Related Work

To the best of our knowledge, learning to simulate human movement is a problem setting that remains largely unexplored. The most similar problem setting in literature is *human mobility prediction* in trajectory data mining [Wang et al., 2019]. Individual mobility models like random walk [Pearson, 1905] mainly characterize the mobility patterns and illustrate a path with a succession of random steps [Song et al., 2010, Brockmann et al., 2006]. Markov-based model is a typical mobility prediction model that learns the location transition probability to predict a future state, based on the assumption that the current user location is related to the previous location [Song et al., 2006, Mathew et al., 2012, Qiao et al., 2014, Terroso-Sáenz et al., 2016]. Recently, deep learning-based methods are widely used for human mobility prediction [Song et al., 2016, Liu et al., 2016,

Feng et al., 2017, Baumann et al., 2018, Feng et al., 2018]. As shown in Figure 1, these mobility prediction has the same objective, which is to minimize the error between estimated  $\hat{s}_{t+1}$  and true observed  $s_{t+1}$ . By mining peoples trajectory data, deep learning-based methods can incorporate spatial and temporal context with the trajectory features and predicts the users next location. *In the problem setting of human mobility prediction, there are often only transitions between states where there is no agent or agents play insignificant roles.* However, in our problem setting, we aim to learn to simulate the state transitions in the human world where intelligent agents (like humans or vehicles with human drivers) play a very significant role where the focused states mostly describe human activities, and the state transition is primarily affected by rational decisions.

In machine learning field, *imitation learning* can be applied to learn the unknown policy  $\pi$  that can generate the movements by taking a sequence of actions  $a$  from  $\pi$  [Abbeel and Ng, 2004, Ziebart et al., 2008, Ross et al., 2011, Ho and Ermon, 2016, Fu et al., 2017]. Recent advances in imitation learning, especially those combining with Generative Adversarial Networks (GAN), have shown successful performance in learning expert policy in applications such as car racing games [Ross et al., 2011] and speech animation [Taylor et al., 2017]. However, *imitation learning often ignores system dynamics.* In our problem setting, both system dynamics  $G$  and policy  $\pi$  considered to model the state transition.

### 3 Preliminaries

In this section, we formally formulate our problem of learning to simulate human movements and then illustrate our definition using an example of a traveler moving in the grid world.

#### 3.1 Problem Formulation

**Definition 1** (State and action). *A state  $s^t$  of an agent describes the surrounding environment of the agent, and the action  $a^t$  is the agent takes at time  $t$  using its policy  $\pi$ , i.e.,  $a^t \sim \pi(a|s^t)$ .*

**Definition 2** (State trajectory and movement trajectory). *A state trajectory of an agent is a sequence of states generated by the agent, usually represented by a series of chronologically ordered pairs, i.e.,  $\xi = (s^{t_0}, \dots, s^{t_T})$ . A movement trajectory of an agent is a chronologically ordered sequence of state-action pairs, i.e.,  $\tau = (\tau^{t_0}, \dots, \tau^{t_T})$  where  $\tau^{t_i} = (s^{t_i}, a^{t_i})$ .*

**Problem 1.** *In our problem setting, we observe a set of state trajectories  $\mathcal{S} = \{\xi_1, \xi_2, \dots, \xi_N\}$  of a real-world system with  $N$  agents. Our goal is to learn the transition function  $f(s^{t+1}|s^t)$  from  $s^t$  to  $s^{t+1}$  so that the error between estimated state  $\hat{s}^{t+1}$  and true state  $s^{t+1}$  is minimized.*

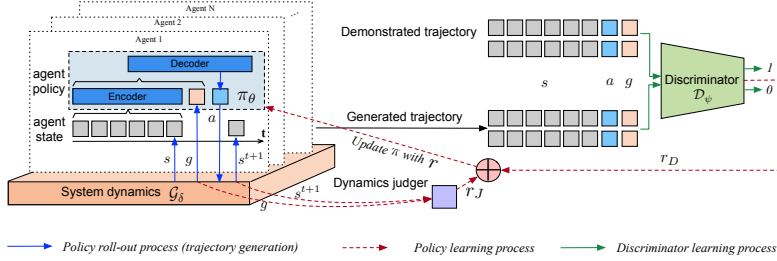


Figure 2: Illustration of the proposed framework. It has four main components: the system dynamics  $\mathcal{G}_\delta$ , the dynamic judger  $J$ , the agent policy  $\pi_\theta$ , and the discriminator  $\mathcal{D}_\psi$ .  $\pi$  and  $\mathcal{G}$  together influences the transition of states. The discriminator learns to differentiate between demonstrated trajectories and generated trajectories and provide reward  $r_D$  for learning policy  $\pi$  that behaves similarly to the true policy. The dynamics judger provides additional intrinsic reward  $r_J$  from the system to the policy, indicating whether the policy behaves compliantly with system constraints. Better viewed in color.

As in Figure 1 (a), traditional supervised learning solutions to this problem learn a direct mapping function  $f_\vartheta$  from  $s^t$  to  $s^{t+1}$  through minimizing some loss function  $\mathcal{L}$  over the set of state trajectories as training data:

$$\underset{\vartheta}{\operatorname{argmin}} \mathbb{E}_{(s^t, s^{t+1}) \sim \mathcal{T}_E} [\mathcal{L}(s^{t+1}, f_\vartheta(s^t))] \quad (1)$$

In this paper, instead of solving this problem through learning a direct mapping from  $s^t$  to  $s^{t+1}$ , we tackle it from a decision-making perspective. As shown in Figure 1 (c), in our problem, an agent observes state  $s^t$  from the system state  $S^t$ , takes action  $a$  following policy  $\pi$  at every time step. System model  $\mathcal{G}$  takes current system states  $S^t$  and the actions  $\{a_1^t, \dots, a_N^t\}$  of all agents as input, and outputs the next system state  $S^{t+1}$ , upon which the agents observes their states  $\{s_1^{t+1}, \dots, s_N^{t+1}\}$ .

## 4 Method

In this section, we first overview the general framework of *MoveSD*; then, we describe each component of the architectures; finally, we introduce the training process and discuss possible paradigms in learning the models.

### 4.1 Overview

As in shown in Figure 2, *MoveSD* has four components, namely the system dynamics  $\mathcal{G}_\delta$ , the dynamic judger  $J$ , the agent policy  $\pi_\theta$ , and the discriminator  $\mathcal{D}_\psi$  to learn to simulate the state transition. We formulate the problem of learning to simulate  $f_{\theta, \delta} = \{\pi_\theta, \mathcal{G}_\delta\}$  to perform real-world-like movements by re-

warding it for “deceiving” the discriminator  $\mathcal{D}_\psi$  trained to discriminate between policy-generated and observed true trajectories.

The system dynamics  $\mathcal{G}_\delta$  takes as input the system state  $S$  and generates the physical constraints  $g$  for each agent, which we parameterize as a multilayer perceptron (MLP). The policy  $\pi_\theta$  takes as input the observed trajectories and the physical constraints  $g^t$  from  $\mathcal{G}_\delta$  and generate an action distribution  $\pi_\theta(a|s)$  and sample an action  $\hat{a}^t$  from the distribution, which we parameterize as a Recurrent Neural Network (RNN):  $\hat{a}^t \sim \pi(a|s^{t-L}, \dots, s^t; g^t)$ , where  $L$  is the observed trajectory length.

The next state  $s^{t+1}$  of the agent can be calculated based on  $s^t$ ,  $\hat{a}^t$  and with system states  $S^t$ . Then the movement trajectories  $\mathcal{T}^G = \{\tau_1, \dots, \tau_N\}$  of  $N$  agents in the system can be generated. The generated trajectories  $\mathcal{T}^G$ , are then fed to 1) the discriminator  $\mathcal{D}_\psi$  to output a score of the probability of the trajectory being true and 2) the dynamics judger  $\mathcal{J}$ , a rule-based calculator, to measure the extent of state  $s$  meeting system physical constraints  $g$ .

The policy  $\pi_\theta$  and discriminator  $\mathcal{D}_\psi$  are jointly optimized through the framework of GAIL [Ho and Ermon, 2016] in the form of an adversarial minimax game as GAN [Goodfellow et al., 2014]:

$$\begin{aligned} \max_{\psi} \min_{\theta} \mathcal{L}(\psi, \theta) = & \mathbb{E}_{(s,a;g) \sim \tau \in \mathcal{T}_E} \log \mathcal{D}_\psi(s, a; g) + \\ & \mathbb{E}_{(s,a;g) \sim \tau \in \mathcal{T}_G} \log(1 - \mathcal{D}_\psi(s, a; g)) - \beta H(\pi_\theta) \end{aligned} \quad (2)$$

where  $\mathcal{T}_E$  and  $\mathcal{T}_G$  are the observed true trajectories and the trajectories generated by  $\pi_\theta$  and  $\mathcal{G}_\delta$  in the environment,  $H(\pi_\theta)$  is an entropy regularization term. Different from the vanilla GAIL whose discriminator is trained with  $(s, a)$ , in this paper, the discriminator is also conditioned on the system constraints as  $\mathcal{D}_\psi(s, a; g)$ .

## 4.2 System Dynamics Design

In this work, we consider the critical factors underlying the agent decision-making process, namely the system constraints  $g$  given by the system dynamics  $\mathcal{G}$ . Specifically for movements on space, *the time for an agent to spend in a location* is particularly crucial in deciding the action of the agent. For example, due to the physical distance between two locations and the travel speed of the agent, it is unlikely for an agent to move arbitrarily from one location to another instantly. Another example is that the time of a traveler staying at a demanding location is influenced by the waiting time to get served.

To approximate these system constraints, we take advantage of the observed trajectories of all agents and use the duration they spend at each location as hindsight for system constraints at the location. Given the trajectories of all agents in the system, we can build training data for system dynamics  $\mathcal{G}_\delta$  by extracting features  $o_g$  for a location and calculating the duration that each agent spent in the location as labels  $g$ . In this paper, we use the location ID, time, the number of agents in the location as features, and employ an MLP to predict the duration an agent stays in the location. To mimic the stochastic

nature of the system dynamics, we sample the constraints  $g$  from a distribution, whose parameters are the outputs of  $\mathcal{G}$ . Specifically, we set the outputs of  $\mathcal{G}$  to be the shaping parameters for Beta distribution:

$$\begin{aligned}
 h_0^g &= \sigma(o_g W_0^g + b_0^g) \\
 h_1^g &= \sigma(h_0^g W_1^g + b_1^g) \\
 &\dots \\
 \Xi &= \sigma(h_{G-1}^g W_G^g + b_G^g) \\
 g &\sim \text{Beta}(\Xi)
 \end{aligned} \tag{3}$$

where  $G$  is the number of layers,  $W_i^g \in \mathbb{R}^{n_{i-1} \times n_i}$ ,  $b_i^g \in \mathbb{R}^{n_i}$  are the learnable weights for the  $i$ -th layer.  $\sigma$  is ReLU function (same denotation for the following part of this paper), as suggested by [Radford et al., 2015]. For  $i = 0$ , we have  $W_0^g \in \mathbb{R}^{c \times n_0}$ ,  $b_0^g \in \mathbb{R}^{n_0}$ , where  $c$  is the feature dimension for  $o_g$  and  $n_0$  is the output dimension for the first layer; for  $i = G$ , we have  $W_G^g \in \mathbb{R}^{n_{G-1} \times 2}$ ,  $b_G^g \in \mathbb{R}^{1 \times 2}$ ,  $\Xi$  is the 2-dimensional shaping parameter for Beta distribution.

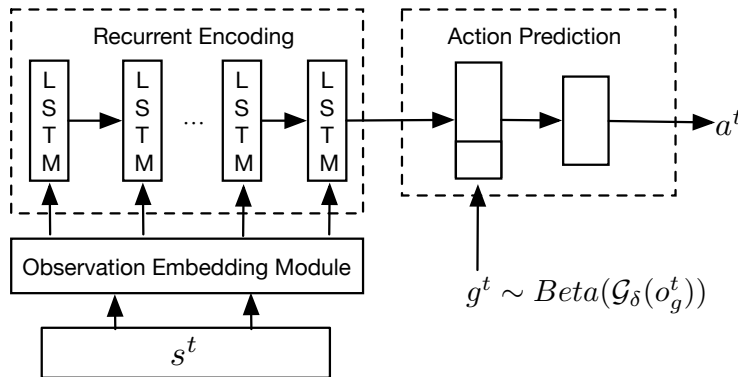


Figure 3: Architecture of policy network  $\pi_\theta$

### 4.3 Policy Design

The architecture of the policy network consists of three major components: 1) observation embedding; 2) recurrent encoding; 3) action prediction, as shown in Figure 3.

#### 4.3.1 Observation Embedding

The architecture of the policy network consists of three major components: 1) observation embedding; 2) recurrent encoding; 3) action prediction, as shown in Figure 3.

Given the raw data of the state observation, *i.e.*, current location the agent is in, time, and other location properties, we first embed the state observation

with a multi-modal embedding module. A simple model like Markov chains can only describe the transitions between independent states like locations. However, mobility transition can be governed by multiple factors like location and time. Thus, we design a multi-modal embedding module to jointly embed the observations into dense representations to help model the complicated transitions.

Specifically, we embed  $k$ -dimensional state features into an  $m$ -dimensional latent space via an embedding layer that copes with location ID  $loc^t$ , a layer of Multi-Layer Perceptron for the rest of the state features  $o^t$  and a concatenation layer on the outputs from previous two layers:

$$\begin{aligned} x^t &= Concat(Embed(loc^t), MLP(o^t)) \\ &= Concat(OneHot(loc^t)W_e, \sigma(o^tW_o + b_o)) \end{aligned} \quad (4)$$

where  $W_e \in \mathbb{R}^{l \times m_1}$ ,  $W_o \in \mathbb{R}^{k \times m_2}$ ,  $b_o \in \mathbb{R}^{m_2}$  are weight matrixes and bias vectors to learn. Here, there are total  $l$  location IDs, and  $m_2 = m - m_1$ . The concatenated state represents the current state of the agent.

### 4.3.2 Recurrent encoding

The policy of the agent should intuitively grasp a fair understanding of the previous states to decide its next action. However, the sequential nature of moving agents poses practical challenges for conventional feed-forward neural policies [Ho and Ermon, 2016, Li et al., 2017] to reason about the status of the agent as well as the dynamic interactions between multiple agents. Towards this end, we propose the policy  $\pi$  with an architecture inspired by the encoder-decoder model [Cho et al., 2014] to account for the sequential nature, as depicted by the recurrent part in Figure 3. To capture the individual status from its past observations, we input the observations of past  $L_{in}$  timesteps to the encoder RNN, one observation per step, which progresses as:  $h_R^i = RNN_{enc}(x^i, h^{i-1}), \forall t - L_{in} \leq i \leq t$ . The last hidden state,  $h_R^t$  is treated as the fixed-length descriptor of past trajectories for the agent.

### 4.3.3 Action prediction

The action prediction module takes  $h_R^t$ , the output of encoder RNN, and the system dynamic constraints  $g^t$  as input. The final action is sampled from the action distribution  $p^A$  with an MLP:

$$\begin{aligned} h_0^A &= Concat(h_R^t, g^t) \\ h_1^A &= \sigma(h_0^A W_1^A + b_1^A) \\ h_2^A &= \sigma(h_1^A W_2^A + b_2^A) \\ &\dots \\ p^A &= Softmax(h_{H-1}^A W_H^A + b_H^A) \\ a^t &\sim Cat(p^A) \end{aligned} \quad (5)$$

where  $W_i^A \in \mathbb{R}^{d_{i-1} \times d_i}$ ,  $b_i^A \in \mathbb{R}^{d_i}$  are the learnable weights for the  $i$ -th layer in action prediction module. For  $i = H$ , we have  $W_H^A \in \mathbb{R}^{n_{H-1} \times |\mathcal{A}|}$ ,  $b_H^A \in \mathbb{R}^{|\mathcal{A}|}$ , where  $|\mathcal{A}|$  is the total number of candidate actions.

#### 4.4 Discriminator and Dynamics Judger

The discriminator network takes a similar network structure as a policy network, with the action prediction module in  $\pi$  replaced by a binary classifier with an MLP. When training  $\mathcal{D}_\psi$ , Equation (2) can be set as a sigmoid cross entropy where positive samples are from observed true trajectories  $\mathcal{T}_E$ , and negative samples are from generated trajectories  $\mathcal{T}_G$ . Then optimizing  $\psi$  can be easily done with gradient ascent on the following loss function:

$$\mathcal{L}_D = \mathbb{E}_{(s,a,g) \in \mathcal{T}_E} \log \mathcal{D}_\psi(s, a; g) + \mathbb{E}_{(s,a,g) \in \mathcal{T}_G} \log(1 - \mathcal{D}_\psi(s, a; g)) \quad (6)$$

The transition between states in a real-world system is an integration of physical rules, control policies, and randomness. Thus its true parameterization is assumed to be unknown. Therefore, given  $\mathcal{T}_G$  generated by  $\pi_\theta$  in the system, Equation (2) is non-differentiable w.r.t  $\theta$  and the gradient cannot be directly backpropagated from  $\mathcal{D}_\psi$  to  $\pi_\theta$ . In order to learn  $\pi_\theta$ , we optimize through policy gradient algorithms in reinforcement learning like TRPO [Schulman et al., 2015] or PPO [Schulman et al., 2017], with a surrogate reward function formulated from Equation (2) as:

$$r_D(s^t, a^t; g^t) = -\log(1 - \mathcal{D}_\psi(s^t, a^t; g^t)) \quad (7)$$

Here, the surrogate reward  $r_D(s^t, a^t, g^t)$  is derived from the discriminator  $\mathcal{D}_\psi$  and can be perceived to be useful in driving  $\pi_\theta$  into regions of the state-action space at time  $t$  similar to those in observations.

**Dynamics judger** In order to make the learned policy behaves realistically, it is necessary to provide guidance to avoid generating trajectories that do not meet the real-world constraints. To explicitly incorporate the system constraints, we draw inspiration from [Ding et al., 2019] and propose a novel intrinsic reward term into the learning of our policy as follows:

$$r_J(s^t, a^t, g^t, s^{t+1}) = \begin{cases} 0, & \text{if } g^t > \Gamma(s^{t+1}) \text{ or } a^t \text{ is not "stay"} \\ \frac{|g^t - \Gamma(s^{t+1})|}{g^t}, & \text{otherwise} \end{cases} \quad (8)$$

where  $\Gamma(s)$  is a pre-defined function that extracts information relatively to  $g$ . Specifically in this paper, we extract *the duration of the agent spent in current location* from state  $s$ , and compare it with the time constraints  $g^t$  from  $\mathcal{G}_\delta$ . Intuitively, when  $\Gamma(s^t) < g^t$ ,  $r_J$  should be positive when the agent takes  $a^t$  of staying in the current location. With such a design, the agent’s action will be

rewarded when it meets the system constraint, and the generated movement is more likely to be a real-world movement.

The final surrogate reward for training  $\pi_\theta$  is defined as follows:

$$r = (1 - \eta) \cdot r_J(s^t, a^t, g^t, s^{t+1}) + \eta \cdot r_D(s^t, a^t, g^t) \quad (9)$$

where  $\eta$  is a hyper-parameter that balances the objective of satisfying the physical constraints and mimics the true trajectories, both of which are pushing the policy learning towards modeling real-world transitions.

## 4.5 Training Process

Since the system constraint  $g$  given by  $\mathcal{G}_\delta$  is used in  $\tau$  when learning  $\pi_\theta$  and  $\mathcal{D}_\psi$ , here we discuss the options in learning  $\mathcal{G}_\delta$ , and investigate their effectiveness empirically in Section 5.6.2:

- **Option 1:** Pre-train  $\mathcal{G}_\delta$  before the learning of  $\pi_\theta$  and  $\mathcal{D}_\psi$  (line 1 in Algorithm 1), fix  $\delta$  during the learning of  $\theta$  and  $\psi$ .
- **Option 2:** At each round of updating  $\pi_\theta$  and  $\mathcal{D}_\psi$ , we update  $\mathcal{G}_\delta$  as well based on the generated trajectories.
- **Option 3:** Integrate the  $\mathcal{G}_\delta$  with  $\pi_\theta$  in one model. The output of  $\mathcal{G}_\delta$  is fed into  $\pi$  before action prediction module. The training of this option would require a model that is optimized through multi-task learning, with one task learns the action prediction and the other task learns to predict  $g$ .

---

### Algorithm 1: Training procedure of *MoveSD*

---

**Input:** Observed true trajectories  $\mathcal{T}_E$ , initial system dynamics, policy and discriminator parameters  $\delta_0, \theta_0, \psi_0$

**Output:** Policy  $\pi_\theta$ , Discriminator  $\mathcal{D}_\psi$ , System dynamics  $\mathcal{G}_\delta$

- 1 Pretrain system dynamics  $\mathcal{G}_\delta$ ;
- 2 **for**  $i \leftarrow 0, 1, \dots$  **do**
- 3     Rollout trajectories for all agents  $\mathcal{T}_G = \{\tau | \tau = (\tau^{t_0}, \dots, \tau^{t_N})\}$ , where  $\tau^t = (s^t, a^t, g^t, s^{t+1})$ ,  $g^t = \mathcal{G}_\delta(o_g^t)$ , and  $a^t \sim \pi_{\theta_i}(s^t, a^t, g^t)$
- 4     # Generator update step
- 5     • Score  $\tau^t$  from  $\mathcal{T}_G^D$  with discriminator, generating reward using Eq. (7);
- 6     • Update  $\theta$  given  $\mathcal{T}_G^D$  by optimizing Eq. (2) with TRPO;
- 7     # Discriminator update step
- 8     • Update  $\psi$  by optimizing Eq. (6)

---

Algorithm 1 describes the training procedure of *MoveSD* with the option of pretraining  $\mathcal{G}_\delta$ . Training *MoveSD* with other options shares almost the same process. We firstly initialize the parameters of  $\mathcal{G}_\delta$ ,  $\pi_\theta$  and  $\mathcal{D}_\psi$  and pre-train  $\mathcal{G}_\delta$ . At each iteration of the algorithm, the policy parameters are used by every agent to generate trajectories  $\mathcal{T}_G$ . Rewards are then assigned to each state-action-goal pair in these generated trajectories. Then the generated trajectories are used to

perform an update on the policy parameters  $\theta_i$  via policy optimization methods TRPO [Schulman et al., 2015]. The generated trajectories  $\mathcal{T}_G$  and observed true trajectories  $\mathcal{T}_E$  are subsequently used as the training data to optimize parameters  $\psi$ .

## 5 Experiment

We aim to answer the following research questions:

- **RQ1:** Compared with baseline methods, can our proposed model *MoveSD* better model the movements of travelers?
- **RQ2:** How does different components (system dynamic model  $\mathcal{G}$ , training paradigm of  $\pi$ , and base RNN model) of *MoveSD* influence the final performance?
- **RQ3:** Can our model generate movements like observed ones?

### 5.1 Experiment Environments and Datasets

We evaluate our method in two real-world travel datasets: the travel behavior data in a theme park and the travel behavior of vehicles in a road network. The state and action definitions for agents in each environment are shown in Table 1.

- **ThemePark.** This is an dataset that contains the tracking information for all visitors to a simulated park. The park covers a large geographic space (approx.  $500 \times 500 m^2$ ) and is populated with ride attractions, restaurants, and food stops, and hosting thousands of visitors each day. All visitors must use a mobile application to check into rides and some other attractions. The mobile application records the location of visitors by a grid ID, where the whole park is divided into  $5m \times 5m$  grid cells. Each data record contains a record time, a traveler ID, a grid ID, and an action. The action is recorded every second when travelers move from grid square to grid square or check-in at attractions.

- **RouteCity.** This is a vehicle trajectory dataset captured from surveillance cameras installed around 25 intersections in Xixi Sub-district at Hangzhou, China. The trajectory of a recorded vehicle includes the timestamp, vehicle ID, road segment ID, and the action of the vehicle. The action can be staying on the current road segment, and transiting to the next road segment by turning left, turning right, taking U-turn, or going straight.

### 5.2 Baselines

We compare with both classical and state-of-the-art methods in human mobility prediction algorithms, including Markov-based methods and deep learning-based methods. We use the same features in deep learning-based methods and our proposed method for a fair comparison.

Table 1: State and action definition for travelers/vehicles in *ThemePark* and *RouteCity*. In *ThemePark*, travelers move between grids; the actions indicate which neighboring grid it travels or stay/check-in in the current grid. In *RouteCity*, vehicles move between road segments, and the actions indicate to stay in the current road or to go to different directions towards its neighboring roads.

Env	Type	Description
<i>ThemePark</i>	Time	Time spent in current grid, start time
	Location	Current grid ID, population in current grid, if current grid checkinable
	Action	Move to eight adjacent grids, stay or check-in in current grid
<i>RouteCity</i>	Time	Time spent in current road, start time
	Location	Current road ID, destinated road, current population in the grid, previous road
	Activity	Last action
	Action	Turn left, turn right, take u-turn, go straight, stay on current road

- **Random Walk** [Brockmann et al., 2006]. This is a classic method that models the movement of agents as a stochastic process, where the agent takes action among all possible actions with equal probability.

- **Markov Model** [Gambis et al., 2012]. The Markov-based method is another representative model to predict human movements. It regards all the visited locations as states and builds a transition matrix to capture the first or higher-order transition probabilities between them. Following existing methods [Feng et al., 2018, Gao et al., 2019], we use the first-order Markov model in our experiment.

- **RNN Model** is widely used to predict the next location by modeling temporal and spatial history movements. In this paper, we use LSTM in [Liu et al., 2016] as the base of our proposed model and as a baseline. Note that since our method can be extended to different deep-learning methods, we further investigate our method with different choices of the base model in Section 5.6.3.

### 5.3 Metrics

To measure the discrepancy between the learned human movements and real-world movements, we evaluate the performance of different methods in the following two tasks:

**Next location prediction** Given the same input states for an agent, a good simulation model should perform well in predicting the next location. Following

Table 2: Performance of different methods in predicting the next location and generating future trajectories w.r.t accuracy (Acc@N), average displacement error (ADE), and final displacement error (FDE). For Acc@N, the higher, the better; for ADE and FDE, the lower, the better. *MoveSD* performs the best against state-of-the-art baselines and its variants.

<i>ThemePark</i>					
	Predicting next location			Generating 1000 steps	
	Acc@1	Acc@3	Acc@5	ADE	FDE
<i>Random Walk</i>	0.120	0.358	0.574	67.291	75.492
<i>Markov Model</i>	0.734	0.788	0.795	45.087	39.768
<i>RNN Model</i>	0.767	0.806	0.871	38.129	34.196
<i>MoveSD wo/ GAIL</i>	0.756	0.847	0.906	21.602	28.762
<i>MoveSD wo/ dynamic</i>	0.771	0.853	0.979	15.634	27.454
<i>MoveSD</i>	<b>0.864</b>	<b>0.892</b>	<b>0.986</b>	<b>9.842</b>	<b>16.716</b>
<i>RouteCity</i>					
	Predicting next location			Generating 1000 steps	
	Acc@1	Acc@3	Acc@5	ADE	FDE
<i>Random Walk</i>	0.192	0.573	1.000 *	1.589	1.644
<i>Markov Model</i>	0.408	0.539	1.000	1.105	1.149
<i>RNN Model</i>	0.7043	0.752	1.000	0.727	0.733
<i>MoveSD wo/ GAIL</i>	0.7587	0.783	1.000	0.724	0.724
<i>MoveSD wo/ dynamic</i>	0.7259	0.959	1.000	0.331	0.625
<i>MoveSD</i>	<b>0.892</b>	<b>0.994</b>	1.000	<b>0.154</b>	<b>0.301</b>

\*Acc@5 in *RouteCity* are all equals to 1 because the maximum number of next candidate locations is 5.

existing studies [Song et al., 2010, Song et al., 2016, Feng et al., 2018], we use the standard evaluation performance metrics, **Acc@k**, which ranks the candidate next locations by the probabilities generated from the model, and check whether the ground-truth location appears in the top  $k$  candidate locations.

**Trajectory generation** Given the same initial states for an agent, a good simulation model should not only perform well in predicting the next location but also be precise in generating the future trajectories as observed ones. Therefore, we also evaluate the performance on generating trajectory to measure the discrepancy between the learned transition model and real transitions, with the following metrics widely used in existing literature [Zou et al., 2018, Lisotto et al., 2019, Liang et al., 2019]:

- **Average Displacement Error (ADE)**: The average of the root mean squared error (RMSE) between the ground truth coordinates  $Y_i^t$  and the predicted coordinates  $\hat{Y}_i^t$  at every timestamp  $t$  for every trajectory  $i$ :  $ADE = \frac{\sum_{i=1}^N \sum_{t=1}^{T_{pred}} \sqrt{(\hat{Y}_i^t - Y_i^t)^2}}{N \cdot T_{pred}}$

- **Final Displacement Error (FDE)**: The average of the RMSE at the final predicted points  $\hat{Y}_i$  and the final true points  $Y_i$  of all trajectories:  $FDE = \frac{\sum_{i=1}^N \sqrt{(\hat{Y}_i - Y_i)^2}}{N}$

Note that for *ThemePark*, since all the grids are evenly divided to  $5m \times 5m$ , we only calculate the differences in horizontal and vertical indexes of grids; for *RouteCity*, we use the midpoint coordinates of road segments when calculating the distances between road segments.

## 5.4 Experimental Settings

In all the following experiments, if not specified, the observed time length  $L_{in}$  is set to be 10. The output length of  $L_{out}$  is 1 for the next location prediction task, and 1000 for trajectory generation task. We fix the length  $L_{in}$  and  $L_{out}$  for simplicity, but our methods can be easily extended to different lengths since the neural networks are recurrent in taking the trajectories as input and in predicting future trajectories. For *ThemePark*, we sample all the trajectories at every second, and for *RouteCity*, we sample the trajectories at every 10 seconds.

We specify some of the important parameters here. For the policy network  $\pi$ , we set the units as 50 for all hidden layers in the recurrent encoding module. For the dynamic system network  $G$ , we use an MLP with two 50-units hidden layers and an output layer with two units as the parameters for a Beta distribution. For discriminator  $\mathcal{D}$ , the output layer has a sigmoid unit.  $\eta$  is set as 0.8.

## 5.5 Overall Performance (RQ1)

In this section, we investigate the performance of our proposed method *MoveSD* on learning the travel movements in two real-world datasets from two perspectives: predicting the next location and generating future trajectories. Table 2 lists the performance of the proposed *MoveSD*, classic models as well as state-of-the-art learning methods in the real-world environments. We have the following observations:

- *MoveSD* achieves consistent performance improvements over state-of-the-art prediction (*RNN Model*) methods across different environments. The performance improvements are attributed to the benefits from the modeling of the decision process with *GAIL* and the integration with system dynamics.
- The performance gap between the proposed *MoveSD* and baseline methods becomes larger in trajectory generation than in the next location prediction. This is because the framework of *GAIL*, which iteratively updates policy  $\pi_\theta$  and discriminator  $\mathcal{D}_\psi$  enables us to model the decision process that determines the whole trajectory effectively. The discriminator in our model can differentiate whether the trajectory is generated or real, which can drive the bad-behaved actions in one iteration to well-behaved ones during the policy learning process of the next iteration.

Table 3: Investigation of different training paradigms for  $\pi$  and  $\mathcal{G}$  in generating trajectories. The lower, the better. Pre-training  $\mathcal{G}$  and jointly learning  $\mathcal{G}$  with  $\pi$  achieves slightly better performance than iteratively updating  $\mathcal{G}$  and  $\pi$ .

Options	<i>ThemePark</i>		<i>RouteCity</i>	
	ADE	FDE	ADE	FDE
#1: Pre-trained $\mathcal{G}$	<b>9.842</b>	<b>16.716</b>	<b>0.154</b>	0.301
#2: $\mathcal{G}$ iteratively trained with $\pi$	13.122	20.970	0.189	0.343
#3: $\mathcal{G}$ and $\pi$ in one model	10.399	17.806	0.160	<b>0.292</b>

## 5.6 Study of *MoveSD* (RQ2)

To get deeper insights on *MoveSD*, we first conduct an ablation study on the modeling of the decision process with *GAIL* and system dynamics  $\mathcal{G}$ . Then we investigate further the impact of system dynamics  $\mathcal{G}$ . Specifically, we examine the influence of different paradigms in training  $\mathcal{G}$  and explore how different base RNN models will influence the *MoveSD* with  $\mathcal{G}$ .

### 5.6.1 Variants of our proposed method

We consider several variations of our model as follows. Note that all the variants share the same neural network structure.

- ***MoveSD* wo/ *GAIL***. This model takes both the state and constraints from system dynamics as its input. It shares the same network structure as *RNN Model*. Different from *MoveSD*, it does not have a discriminator to conducting adversarial training. Instead, it is trained with supervised learning. It can also be seen as *RNN Model* methods with information from system dynamics as extra features.
- ***MoveSD* wo/ *dynamic***. This method uses *GAIL* but does not consider the system dynamics. That is, the input of the policy and discriminator do not contain  $g$  from system dynamic model  $\mathcal{G}$ .
- ***MoveSD***. This is our final method, which uses the adversarial learning process as *GAIL*, and considers the system dynamic.

Table 2 shows the performance of variants of our method: *MoveSD* outperforms both *MoveSD* wo/ *dynamic* and *MoveSD* wo/ *GAIL*, indicating the effectiveness of using *GAIL* and the system dynamics. We also notice that *MoveSD* wo/ *GAIL* outperforms pure *RNN Model* in most cases. This is because *MoveSD* wo/ *GAIL* has extra information on the constraints from system dynamics within the model, which validates the effectiveness of considering system dynamics. In the rest of our experiments, we only compare *MoveSD* with other methods.

### 5.6.2 Different training paradigms of $\mathcal{G}$

As mentioned in Section 4.5,  $\pi$  can be trained in different ways with regards to  $\mathcal{G}$ : 1) *pre-trained*  $\mathcal{G}$ , 2)  $\mathcal{G}$  *iteratively trained* with  $\pi$ , or 3)  $\mathcal{G}$  *jointly learned* with  $\pi$  in one model. And the results in Table 3 show that *MoveSD* with pre-training

$\mathcal{G}$  achieves similar performance with using one model integrating both  $\mathcal{G}$  and  $\pi$ , but outperforms training  $\mathcal{G}$  and  $\pi$  iteratively. The reason could be that if the errors for predicting  $g$  from  $\mathcal{G}$  is large in the current iteration and if the errors cannot propagate back to the learning of  $\pi$ ,  $\pi$  taking  $g$  from  $\mathcal{G}$  would lead to further error. Therefore, a good start of  $\mathcal{G}$  through pre-training or using one model to learn both  $\mathcal{G}$  and  $\pi$  can lead to relatively better performance. In the rest of the experiments, we only use pre-trained  $\mathcal{G}$  in *MoveSD* and compare it with other baseline methods.

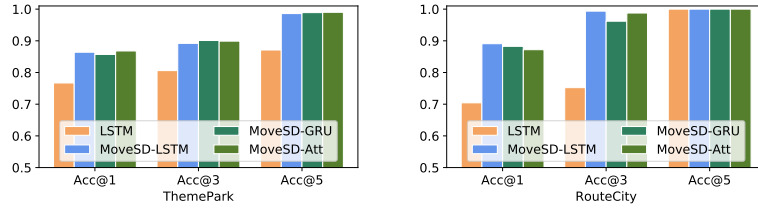
### 5.6.3 Different base models in $\pi$

In the existing literature, different RNN models have been utilized. In this section, we explore the impact of base RNN models in  $\pi$ , and consider the variants of *MoveSD* that use different settings - more specifically, GRU as in [Gao et al., 2019], attentional RNN as in [Feng et al., 2018], and LSTM as in [Liu et al., 2016], termed *MoveSD-GRU*, *MoveSD-Att*, and *MoveSD-LSTM* respectively. Figure 4 summarizes the experimental results, and we have the following findings:

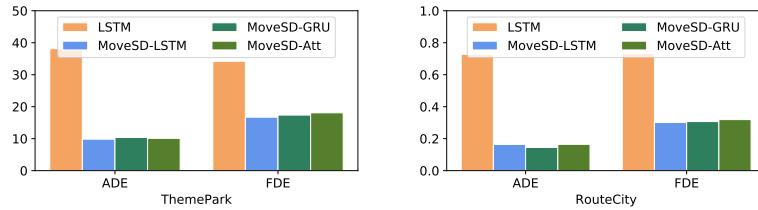
- Our proposed method performs steadily under different base models across various tasks, indicating the idea of our method is valid across different base models. In the rest of our experiments, we use LSTM as our base model and compare it with other baseline methods.
- Our proposed method with different base models performs consistently better than the baseline method *RNN Model*, which uses LSTM. This is because our method not only learns to model the behavior but also considers the influence of system dynamics.

## 5.7 RQ3: Case Study

In this section, we showcase the trajectory of a vehicle generated by different methods under *RouteCity*, as is shown in Figure 5. Blue lines are the true observed trajectories of the vehicle, where we can see the observed vehicle starts traveling at the 320 seconds, passing through two road segments toward its destination (red star) and only reaches at  $C$  at the 1000 second. It spends a certain time on each road, due to the physical length of roads and the travel speed on the road. The red lines indicate the trajectory generated by different methods. We can see that only *MoveSD* can generate a similar trajectory as observed, while all other baselines generate unrealistic trajectories. Specifically, since *RNN Model* yields inaccurate predictions when encountering a new state and the generated trajectory drifts away eventually because of the accumulated inaccuracy in previous predictions. On the other hand, *MoveSD* explicitly models the mechanism behind state transitions and learns to generate trajectories with physical constraints.



(a) Accuracy of location prediction in *ThemePark* and *RouteCity*



(b) Error of trajectory generation in *ThemePark* and *RouteCity*

Figure 4: Performance of *MoveSD* under with different base models, compared with *RNN Model* (LSTM). Up: accuracy of next location prediction under both scenarios. The higher, the better. Down: error of trajectory generation under both scenarios. The lower, the better. *MoveSD* still with different base models outperforms *RNN Model*.

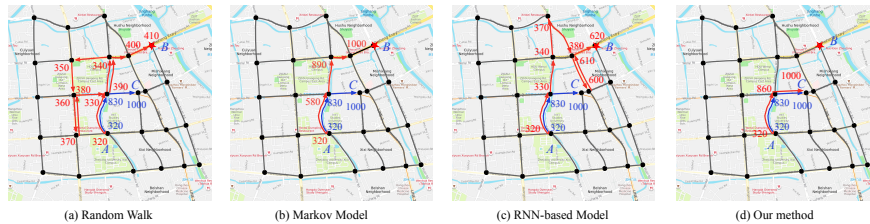


Figure 5: A case study on a vehicle's movement in the first 1000 seconds. All the methods take the same initial information that the vehicle starts its movement at location *A* at the 320 second, and its destination is location *B* (shown as the red star). The numbers next to the nodes are the time of vehicles arriving at corresponding intersections. The blue lines are the true observed trajectories of the vehicle, where it only reaches *C* at the 1000 second. The red lines in different figures indicate the trajectories generated by different methods. Only *MoveSD* can generate a similar trajectory as observed.

## 6 Conclusion

In this paper, we propose to model the state transition of human movement on space as a decision process and learns the decision making policy with system dynamics. Specifically, we propose to integrate the constraints from the

system dynamic model to help the learned state transition more realistic. Extensive experiments on real-world data demonstrate that our method can not only accurately predict the next state of agents, but also accurately generate longer-term future movements.

We want to point out several important future directions to make the method more applicable to the real world. First, the constraints from the system dynamics can include more factors, like the relationship between multiple agents. Second, the raw data for observation only include the status of travelers or vehicles and the location information. More exterior data, like weather conditions, might help to boost model performance.

## References

- [Abbeel and Ng, 2004] Abbeel, P. and Ng, A. Y. (2004). Apprenticeship learning via inverse reinforcement learning. In *ICML'14*.
- [Baumann et al., 2018] Baumann, P., Koehler, C., Dey, A. K., and Santini, S. (2018). Selecting individual and population models for predicting human mobility. *IEEE TMC*.
- [Bhattacharyya et al., 2018] Bhattacharyya, R. P., Phillips, D. J., et al. (2018). Multi-agent imitation learning for driving simulation. In *IROS'18*.
- [Brockmann et al., 2006] Brockmann, D., Hufnagel, L., and Geisel, T. (2006). The scaling laws of human travel. *Nature*, 439(7075):462–465.
- [Cho et al., 2014] Cho, K., Van Merriënboer, B., Gulcehre, C., Bahdanau, D., Bougares, F., Schwenk, H., and Bengio, Y. (2014). Learning phrase representations using rnn encoder-decoder for statistical machine translation. *arXiv:1406.1078*.
- [Ding et al., 2019] Ding, Y., Florensa, C., Abbeel, P., and Phielipp, M. (2019). Goal-conditioned imitation learning. In *NeurIPS'19*.
- [Dulac-Arnold et al., 2019] Dulac-Arnold, G., Mankowitz, D., and Hester, T. (2019). Challenges of real-world reinforcement learning. *arXiv:1904.12901*.
- [Feng et al., 2018] Feng, J., Li, Y., Zhang, C., Sun, F., Meng, F., Guo, A., and Jin, D. (2018). Deepmove: Predicting human mobility with attentional recurrent networks. In *The World Wide Web Conference*, pages 1459–1468.
- [Feng et al., 2017] Feng, S., Cong, G., An, B., and Chee, Y. M. (2017). Poi2vec: Geographical latent representation for predicting future visitors. In *AAAI'17*.
- [Fu et al., 2017] Fu, J., Luo, K., and Levine, S. (2017). Learning robust rewards with adversarial inverse reinforcement learning. *arXiv:1710.11248*.

- [Gambs et al., 2012] Gambs, S., Killijian, M.-O., and del Prado Cortez, M. N. (2012). Next place prediction using mobility markov chains. In *Proceedings of the First Workshop on Measurement, Privacy, and Mobility*, page 3. ACM.
- [Gao et al., 2019] Gao, Q., Zhou, F., Trajcevski, G., Zhang, K., Zhong, T., and Zhang, F. (2019). Predicting human mobility via variational attention. In *The World Wide Web Conference*, pages 2750–2756. ACM.
- [Goodfellow et al., 2014] Goodfellow, I., Pouget-Abadie, J., Mirza, M., Xu, B., Warde-Farley, D., Ozair, S., Courville, A., and Bengio, Y. (2014). Generative adversarial nets. In *NeurIPS’14*.
- [Ho and Ermon, 2016] Ho, J. and Ermon, S. (2016). Generative adversarial imitation learning. In *NeurIPS’16*.
- [Li et al., 2017] Li, Y., Song, J., and Ermon, S. (2017). Inferring the latent structure of human decision-making from raw visual inputs. *arXiv:1703.08840*.
- [Lian et al., 2014] Lian, D., Zhao, C., Xie, X., Sun, G., Chen, E., and Rui, Y. (2014). Geomf: joint geographical modeling and matrix factorization for point-of-interest recommendation. In *KDD’14*.
- [Liang et al., 2019] Liang, J., Jiang, L., Niebles, J. C., Hauptmann, A. G., and Fei-Fei, L. (2019). Peeking into the future: Predicting future person activities and locations in videos. In *CVPR’19*.
- [Lisotto et al., 2019] Lisotto, M., Coscia, P., and Ballan, L. (2019). Social and scene-aware trajectory prediction in crowded spaces. In *Proceedings of the IEEE International Conference on Computer Vision Workshops*.
- [Liu et al., 2016] Liu, Q., Wu, S., Wang, L., and Tan, T. (2016). Predicting the next location: A recurrent model with spatial and temporal contexts. In *AAAI’16*.
- [Mathew et al., 2012] Mathew, W., Raposo, R., and Martins, B. (2012). Predicting future locations with hidden markov models. In *Proceedings of the 2012 ACM conference on ubiquitous computing*, pages 911–918.
- [Pearson, 1905] Pearson, K. (1905). The problem of the random walk. *Nature*, 72(1867).
- [Qiao et al., 2014] Qiao, S., Shen, D., Wang, X., Han, N., and Zhu, W. (2014). A self-adaptive parameter selection trajectory prediction approach via hidden markov models. *IEEE TITS*.
- [Radford et al., 2015] Radford, A., Metz, L., and Chintala, S. (2015). Unsupervised representation learning with deep convolutional generative adversarial networks. *arXiv:1511.06434*.

- [Ross et al., 2011] Ross, S., Gordon, G., and Bagnell, D. (2011). A reduction of imitation learning and structured prediction to no-regret online learning. In *AISTATS'11*.
- [Schulman et al., 2015] Schulman, J., Levine, S., Moritz, P., Jordan, M. I., and Abbeel, P. (2015). Trust region policy optimization. In *ICML'15*.
- [Schulman et al., 2017] Schulman, J., Wolski, F., Dhariwal, P., Radford, A., and Klimov, O. (2017). Proximal policy optimization algorithms. *arXiv:1707.06347*.
- [Song et al., 2010] Song, C., Qu, Z., Blumm, N., and Barabási, A.-L. (2010). Limits of predictability in human mobility. *Science*, 327(5968):1018–1021.
- [Song et al., 2018] Song, J., Ren, H., Sadigh, D., and Ermon, S. (2018). Multi-agent generative adversarial imitation learning. In *NeurIPS'18*.
- [Song et al., 2006] Song, L., Kotz, D., Jain, R., and He, X. (2006). Evaluating next-cell predictors with extensive wi-fi mobility data. *IEEE TMC*.
- [Song et al., 2016] Song, X., Zhang, Q., Sekimoto, Y., Shibasaki, R., Yuan, N. J., and Xie, X. (2016). Prediction and simulation of human mobility following natural disasters. *ACM TIST*.
- [Taylor et al., 2017] Taylor, S., Kim, T., Yue, Y., Mahler, M., Krahe, J., Rodriguez, A. G., Hodgins, J., and Matthews, I. (2017). A deep learning approach for generalized speech animation. *ACM TOG*, 36(4).
- [Terroso-Sáenz et al., 2016] Terroso-Sáenz, F., Cuenca-Jara, J., González-Vidal, A., and Skarmeta, A. F. (2016). Human mobility prediction based on social media with complex event processing. *International Journal of Distributed Sensor Networks*, 12(9):5836392.
- [Wang et al., 2017] Wang, J., Chen, C., Wu, J., and Xiong, Z. (2017). No longer sleeping with a bomb: a duet system for protecting urban safety from dangerous goods. In *KDD'17*.
- [Wang et al., 2019] Wang, J., Kong, X., Xia, F., and Sun, L. (2019). Urban human mobility: Data-driven modeling and prediction. *SIGKDD Explor. Newsl.*
- [Wang et al., 2018] Wang, J., Wang, X., and Wu, J. (2018). Inferring metapopulation propagation network for intra-city epidemic control and prevention. In *KDD'18*.
- [Wei et al., 2018] Wei, H., Zheng, G., Yao, H., and Li, Z. (2018). Intellilight: A reinforcement learning approach for intelligent traffic light control. In *KDD'18*.
- [Wu et al., 2018] Wu, C., Bayen, A. M., and Mehta, A. (2018). Stabilizing traffic with autonomous vehicles. In *ICRA'18*, pages 1–7. IEEE.

- [Ziebart et al., 2008] Ziebart, B. D., Maas, A. L., Bagnell, J. A., and Dey, A. K. (2008). Maximum entropy inverse reinforcement learning. In *AAAI'08*.
- [Zou et al., 2018] Zou, H., Su, H., Song, S., and Zhu, J. (2018). Understanding human behaviors in crowds by imitating the decision-making process. In *AAAI'18*.